

LangMap: A Hierarchical Benchmark for Open-Vocabulary Goal Navigation

Bo Miao¹, Weijia Liu², Jun Luo³, Lachlan Shinnick¹, Jian Liu³, Thomas Hamilton-Smith¹, Yuhe Yang⁴, Zijie Wu⁵, Vanja Videnovic⁶, Feras Dayoub¹, Anton van den Hengel¹

¹AIML, Adelaide University ²East China Normal University ³NERC-RVC, Hunan University
⁴University Western Australia ⁵Singapore University of Technology and Design ⁶Breaker Industries

Project page: bo-miao.github.io/LangMap

Abstract

The relationships between objects and language are fundamental to meaningful communication between humans and AI, and to practically useful embodied intelligence. We introduce HieraNav, a multi-granularity, open-vocabulary goal navigation task where agents interpret natural language instructions to reach targets at four semantic levels: *scene*, *room*, *region*, and *instance*. To this end, we present *Language as a Map (LangMap)*, a large-scale benchmark built on real-world 3D indoor scans with comprehensive human-verified annotations and tasks spanning these levels. LangMap provides *region labels*, *discriminative region descriptions*, *discriminative instance descriptions* covering 414 object categories, and over 18K navigation tasks. Each target features both concise and detailed descriptions, enabling evaluation across different instruction styles. LangMap achieves superior annotation quality, outperforming GOAT-Bench by 23.8% in discriminative accuracy using 4× fewer words. Comprehensive evaluations of strong zero-shot and supervised models on LangMap reveal that richer context and memory improve success, while long-tailed, small, context-dependent, and distant goals, as well as multi-goal completion, remain challenging. HieraNav and LangMap establish a rigorous testbed for advancing language-driven embodied navigation.

1. Introduction

Goal-oriented navigation (GN) is fundamental to embodied intelligence, underpinning applications such as home-assistant robots. It requires agents to comprehend user instructions, *e.g.*, object categories [1, 2] or reference images [3, 4], and to perceive and reason within 3D environments to reach goals without step-by-step guidance. We focus on language-conditioned goal navigation (LGN), which enables intuitive and scalable human-robot interaction.

Previous LGN research has primarily focused on object-

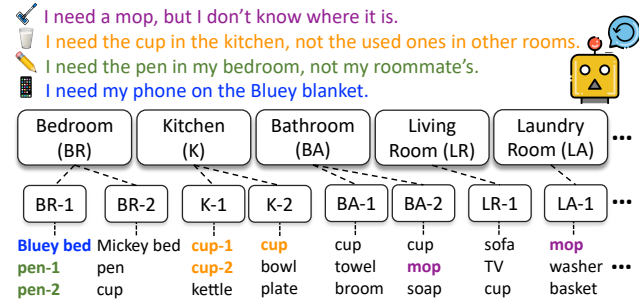


Figure 1. HieraNav requires agents to interpret natural language and navigate to goals across four semantic levels: *scene*, *room*, *region*, and *instance*, where success means reaching a target that satisfies the instruction. Instruction-relevant targets are color-coded.

goal navigation, where agents locate *any* instance of a given category (*e.g.*, chair). Early benchmarks [2, 5] consider 6–21 common object categories and evaluate generalization to new environments. To improve scalability, HM3D-OVON [1] introduces an open-vocabulary setting with 178 categories for evaluation, while LHPV-VLN [6] incorporates heuristically inferred room types. However, category-level navigation prioritizes perception and detection over semantic reasoning. This remains insufficient for real-world scenarios, where users specify context-dependent goals, such as *find the phone on the bed with a Bluey blanket*, that require fine-grained semantic and spatial understanding for disambiguation (see Fig. 1).

Recently, GOAT [7] and PSL [8] have attempted to unify category- and instance-level navigation by leveraging vision-language models to automatically generate instructions from HM3D object views [9, 10]. However, current VLMs often fail to capture distinctive cues [11] and exhibit limited spatial reasoning [12–15], resulting in descriptions that lack uniqueness and reliable spatial grounding. To assess the quality of these auto-generated instructions, we analyze same-category instances within each scene of GOAT-Bench [7] and examine whether the descriptions

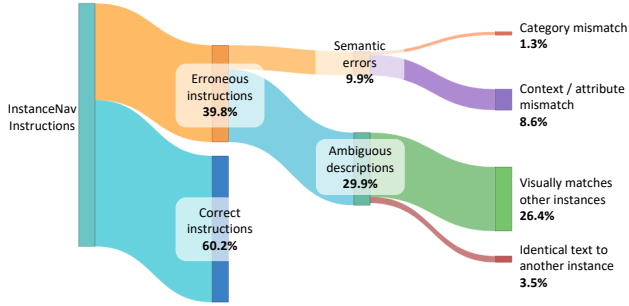


Figure 2. Analysis of instance-level instructions in GOAT-Bench.

are visually grounded and discriminative. As shown in Fig. 2, our manual inspection of ten scenes (around 30% of the evaluation set) reveals that 39.8% of instance-level instructions contain semantic errors (9.9%) or ambiguities (29.9%), where supposedly “unique” instance descriptions match multiple objects or exhibit nearly identical wording (see supplementary materials for examples). These findings expose the limitations of current VLM-based pipelines in generating accurate and unambiguous instructions for semantic navigation. In addition, tasks requiring spatial disambiguation across rooms or regions remain unexplored due to the lack of quality semantic annotations.

To address these limitations, we argue that a robust LGN benchmark should: (i) cover a broad spectrum of goal granularities, from coarse scene-level to fine-grained instance-level; (ii) provide human-verified and discriminative descriptions that uniquely identify targets within each scene; and (iii) support open-vocabulary evaluation for both single-goal tasks at different semantic levels and multi-goal episodes with mixed-level goals.

We introduce **HieraNav**, a multi-granularity open-vocabulary navigation task that unifies goals across four semantic levels: *scene*, *room*, *region*, and *instance*. As shown in Fig. 1, these levels capture the essential granularities of indoor navigation and reflect the diversity of real-world goal specifications. HieraNav requires agents to interpret natural language instructions, perform spatiotemporal reasoning, and navigate to targets aligned with user intent. To enable rigorous evaluation, we present Language as a Map (**LangMap**), a large-scale benchmark built on real-world HM3D scans [9, 10], augmented with *comprehensive, human-verified semantic annotations and navigation tasks across all four semantic levels*. Unlike prior datasets, LangMap provides region labels, discriminative region descriptions (absent from prior benchmarks), and discriminative instance descriptions covering 414 object categories (3.5 \times more than the VLM-generated annotations in GOAT-Bench [7]), along with over 18k navigation tasks. Annotations are created via a *rigorous contrastive protocol* in which annotators compare all same-category regions and

instances within each scene to compose unambiguous descriptions, which are further cross-validated for accuracy. Each target features both concise descriptions emphasizing salient cues and detailed descriptions providing richer context, enabling evaluation across different instruction styles.

We conduct qualitative and quantitative analyses on LangMap, demonstrating superior annotation quality and outperforming GOAT-Bench by 23.8% in discriminative accuracy using 4 \times fewer words. We further evaluate zero-shot and supervised models on LangMap, showing that while richer context and memory improve navigation success, long-tailed, small, context-dependent, and distant goals, as well as multi-goal completion, remain challenging. HieraNav and LangMap establish a rigorous and unified testbed for advancing language-driven embodied navigation. Our main contributions are as follows:

- We introduce HieraNav, a multi-granularity open-vocabulary navigation task that unifies goals across four semantic levels: scene, room, region, and instance, to advance context-aware embodied navigation.
- We present LangMap, a large-scale benchmark built on real-world 3D scans with comprehensive human-verified annotations, including region labels and discriminative region- and instance-level descriptions in concise and detailed forms. It spans diverse object categories and multi-level navigation tasks, delivering high-quality annotations that achieve 23.8% higher discriminative accuracy than GOAT-Bench.
- We evaluate strong zero-shot and supervised models on LangMap, analyzing performance across semantic granularities, instruction styles, long-tailed categories, object sizes, navigation distances, and sequential tasks to uncover key challenges and reasoning limitations.

2. Related Work

Goal-oriented Navigation enables embodied agents to interpret instructions and navigate 3D environments to reach goals. Unlike vision-and-language navigation [16–18], GN is starting-point independent and requires agents to explore and localize goals without step-by-step guidance. Existing GN tasks specify targets in various formats, such as point coordinates [19–22], object categories [1, 2, 5, 23–28], reference images [3, 4, 29–31], or VLM-generated instance descriptions [7, 8], typically focusing on category- or instance-level targets. GN methods generally follow two paradigms: end-to-end reinforcement learning and modular architectures. End-to-end reinforcement learning approaches [32–38] learn representations that map inputs to low-level actions but often suffer from low sample efficiency and poor interpretability. Modular architectures [20, 39–42] decompose navigation into specialized components and construct explicit scene representations, such as scene

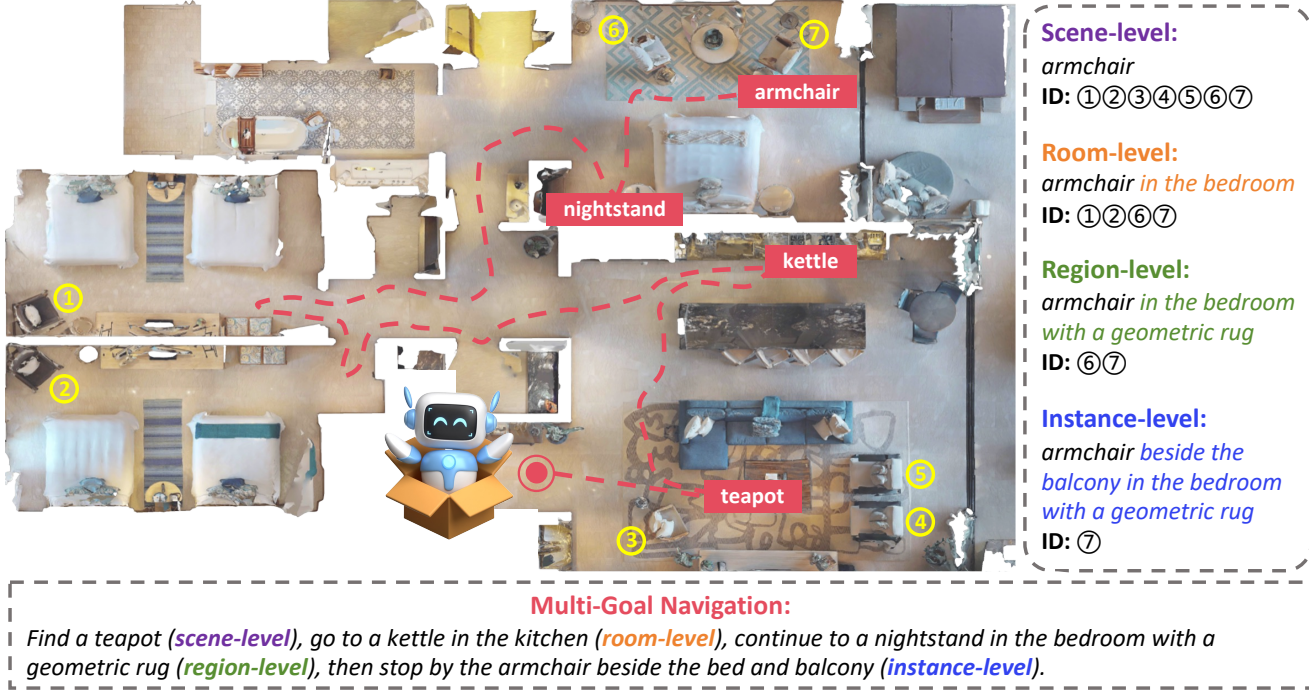


Figure 3. HieraNav requires agents to interpret natural language instructions and navigate to scene-, room-, region-, and instance-level targets. LangMap establishes the first large-scale benchmark for rigorous and systematic evaluation, featuring single-goal tasks at different semantic levels and multi-goal tasks across mixed levels. Target descriptions incorporate intrinsic attributes, spatial-relational context, and open-world semantics.

graphs [43] or top-down maps [44, 45]. Recent advances in VLMs [46–50] further enable zero-shot, open-vocabulary navigation [6, 26, 51–56], leveraging strong multimodal alignment and broad open-world knowledge.

Despite these advances, prior work overlooks language-conditioned goals across multiple semantic levels. We introduce a unified multi-granularity open-vocabulary goal navigation task where agents interpret natural-language goals at four semantic levels: scene, room, region, and instance. This design captures key granularities of indoor navigation and reflects the diversity of real-world goal specifications, enabling natural language goal expression and practical, intuitive embodied navigation.

Language-conditioned Goal Navigation Benchmarks. Early LGN benchmarks [2, 5] utilize real-world scans [5, 9, 10] but include only 6–21 common object categories and primarily evaluate generalization to unseen environments. To increase scene diversity, ProcTHOR [58] generates floor plans populated with 3D assets, and OVMM [59] curates human-authored interactive synthetic scenes. However, these synthetic environments often lack realism and suffer from sim-to-real transfer challenges [60]. To expand object diversity, HM3D-OVON [1] presents an open-vocabulary benchmark with 178 categories for evaluation. LHPN-VLN [6] incorporates heuristically inferred room

types for long-horizon tasks. Nonetheless, these benchmarks emphasize object detection with limited higher-level semantic reasoning.

To enable instance-level goals, GOAT [7] and PSL [8] use VLMs to generate instructions from object views. However, VLMs struggle to capture distinctive visual–semantic cues [11] and exhibit limited 3D spatial reasoning [12–14], resulting in ambiguous or inaccurate descriptions. To address these limitations, we introduce a large-scale benchmark built on real-world 3D scans with comprehensive human-verified semantic annotations. Our benchmark includes both single- and multi-goal navigation tasks across four semantic levels (scene, room, region, and instance) and covers 414 object categories for rigorous and systematic evaluation.

3. Multi-Granularity Open-Vocabulary Goal Navigation

3.1. HieraNav

As shown in Fig. 3, HieraNav requires a mobile agent, randomly initialized in a 3D environment, to perform either single-goal or multi-goal navigation. Although primarily designed for unseen environments, the task also extends to known scenes. Unlike prior work [1, 7, 8], goals are speci-

Table 1. Dataset statistics of popular goal-oriented navigation evaluation benchmarks. \dagger : GOAT-Bench uses VLM-generated descriptions without human verification, resulting in inaccurate and non-discriminative descriptions. LHPN-VLN adds heuristically inferred room types to object categories, and its region-based goal assignment overlooks distinct regions of the same room type, leading to suboptimal evaluation. *Description*: text that uniquely identifies a target instance within a scene. *Small Obj.*: percentage of objects with mean IoU below 3.3%, computed over the agent’s optimal look-up, forward, and look-down views. LangMap provides comprehensive human-verified annotations, such as natural and discriminative region and instance descriptions essential for HieroNav. We report average word counts for both styles; concise instance descriptions average 5.3 words, balancing practical utility with increased navigational challenge.

Evaluation Benchmark	Task Semantic Levels				Region Annotations			Object/Instance Annotations			Small Obj.	Tasks
	Scene	Room	Region	Instance	Category	Description	Words	Category	Description	Words		
RoboTHOR [57]	✓	✗	✗	✗	✗	✗	✗	12	✗	✗	-	-
ObjectNav-MP3D [5]	✓	✗	✗	✗	✗	✗	✗	21	✗	✗	-	-
ObjectNav-HM3D [2]	✓	✗	✗	✗	✗	✗	✗	6	✗	✗	-	-
HM3D-OVON [1]	✓	✗	✗	✗	✗	✗	✗	178	✗	✗	4.2%	9000
LHPN-VLN [6]	✗	✓ [†]	✗	✗	10	✗	✗	-	✗	✗	-	960
GOAT-Bench [7]	✓	✗	✗	✓ [†]	✗	✗	✗	119	1506 [†]	29.0	4.9%	7951
LangMap (Ours)	✓	✓	✓	✓	12	926	5.7/21.0	414	7510	5.3/15.9	22.2%	18479

fied in natural language across four semantic levels:

- *Scene-level*: any object of the target category in the scene (e.g., “*armchair*”).
- *Room-level*: an object of the target category located in a specified room type (e.g., “*armchair in the bedroom*”).
- *Region-level*: an object of the target category within a specific room instance, disambiguated from other rooms of the same type by contextual cues (e.g., “*armchair in the bedroom with a geometric rug*”).
- *Instance-level*: a unique object instance identified by discriminative attributes or contextual relations (e.g., “*armchair beside the bed and balcony*,” “*square coffee table*,” and “*white bed with teal runner*”).

At each time step t , the agent receives an RGB image I_t , depth D_t , and odometry $P_t = (\Delta x, \Delta y, \Delta \theta)$ relative to the start position. The agent is required to reach the goal G specified by natural language instructions. Following standard protocols [1, 7, 8], the action space includes MOVE_FORWARD (0.25m), TURN_LEFT or TURN_RIGHT (30°), LOOK_UP or LOOK_DOWN (30°), and STOP. A task is successful if the agent executes STOP within 1m of any object matching the goal description within 500 steps. The simulated agent follows the physical specifications of the Stretch robot [61]: height 1.41m, base radius 0.17m, and an RGB-D camera mounted at 1.31m.

3.2. LangMap Statistics

LangMap is built on real-world HM3D scans [9, 10] and includes all 36 HM3D-Sem validation scenes. It provides comprehensive human-verified annotations and navigation tasks across four semantic levels, enabling systematic and rigorous evaluation. Table 1 reports detailed statistics, showing that LangMap offers *greater annotation and navigation task diversity, higher annotation quality, and larger scale* than existing benchmarks.

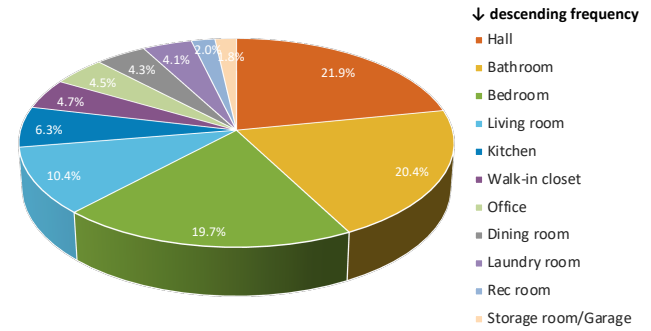


Figure 4. Distribution of region labels in descending frequency.

Region Annotations. Unlike prior datasets limited to object annotations, our LangMap provides human-verified region labels for 12 room categories (Bathroom, Bedroom, Dining room, Garage, Hall, Kitchen, Laundry room, Living room, Office, Recreation room, Storage room, and Walk-in closet) and 926 discriminative region descriptions. These annotations underpin room- and region-level navigation tasks and facilitate scene understanding. Fig. 4 shows the distribution of region labels in LangMap, where most regions correspond to common indoor spaces such as halls, bathrooms, and bedrooms, while recreation rooms, storage rooms, and garages are less frequent.

Object Diversity. LangMap covers 414 object categories, **3.5** \times that of the GOAT-Bench val split (119) and **1.6** \times that of the *full* GOAT-Bench (261), enabling more semantically diverse evaluation. Compared to [1, 7], it also includes more small-object categories (e.g., calculator, mouse, dumbbell) and retains small instances as targets, resulting in a more realistic and challenging setting. Instance counts per category are shown in Fig. 6(a), and the full category list is provided in the supplementary material.

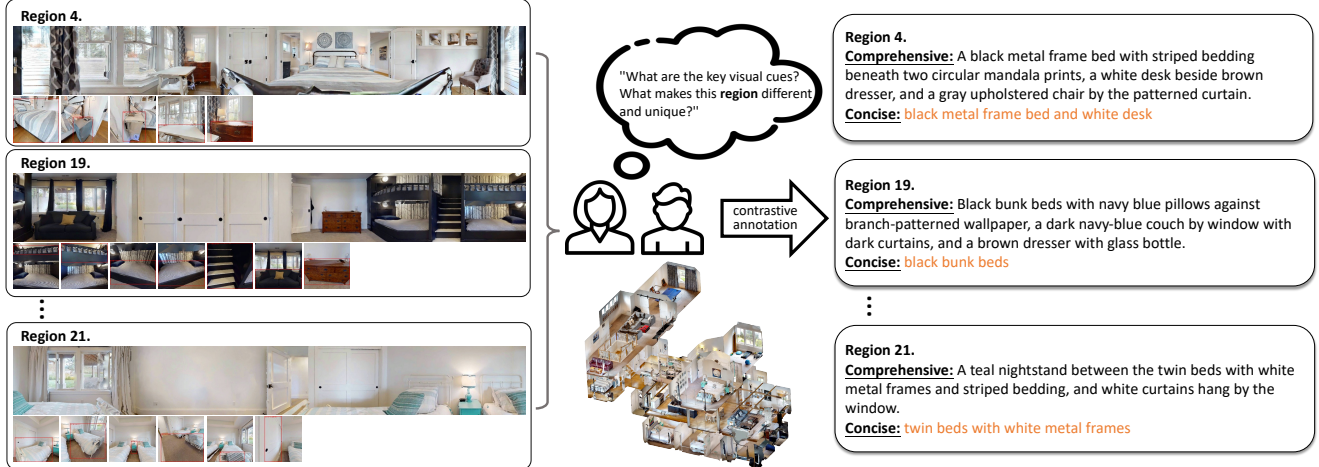


Figure 5. Contrastive region annotation. Annotators are provided with region panoramas, corresponding labeled object views, and 3D scene models to compose one concise and one comprehensive description per region, distinguishing it from other same-category regions via visual comparison. A subsequent cross-check ensures clarity and quality.

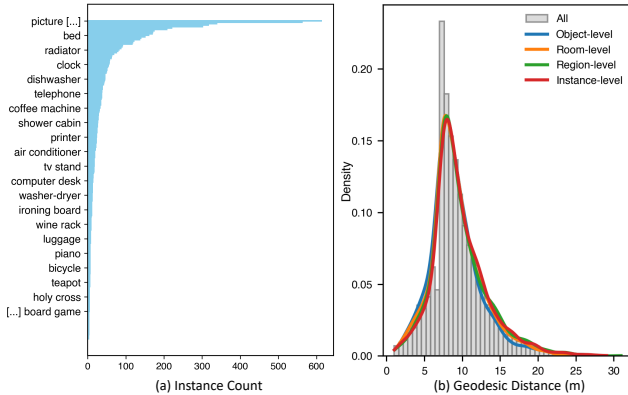


Figure 6. Distribution analysis of LangMap. (a) Instance count per object category (sampled category names shown for readability). (b) Ground-truth geodesic distance distribution for navigation tasks across the four semantic levels.

Instance Annotations. LangMap provides concise and detailed discriminative descriptions created through rigorous contrastive human annotation. In contrast, GOAT-Bench [7] relies on VLM-generated descriptions that often contain semantic errors and lack discrimination (see Fig. 2). In LangMap, concise instance descriptions average only **5.3** words, providing minimal yet sufficient cues to identify target instances. This aligns with real-world goal specification and promotes practical and efficient human–robot interaction.

Task Granularity. LangMap includes single- and multi-goal tasks spanning four semantic levels—*scene*, *room*, *region*, and *instance*—enabling evaluation of exploration, memory, and semantic reasoning. As shown in Fig. 6(b), we align ground-truth geodesic path length distributions for

tasks across semantic levels during task generation, with most tasks having shortest-path distances between 5–15m.

Together, these human-verified, large-scale, and semantically rich annotations establish LangMap as a rigorous testbed for language-conditioned goal navigation.

3.3. Contrastive Region Annotation

LangMap provides human-verified annotations to support room- and region-level goal specification. For each object instance, we sample candidate viewpoints and select the one with the highest visible coverage as its representative view. For each region, we collect the 3D coordinates of all contained objects from HM3D-Sem [10], compute a pseudo-center as the midpoint of the minimum and maximum coordinates, and capture a panoramic observation at this location. Annotators use these region panoramas and object views for room category labeling. Regions spanning multiple room types (e.g., a living room connected to a kitchen) receive all applicable labels.

We then employ a contrastive annotation protocol to derive natural and discriminative region descriptions. As shown in Fig. 5, annotators compare all same-category regions within each scene and write concise and detailed descriptions that identify the target region, where the detailed version extends the concise one with additional attributes. VLM-generated descriptions [62] serve as optional references to streamline the process. A second round of cross-checking ensures quality.

3.4. Contrastive Instance Annotation

Similar to region annotation, we employ a contrastive protocol to derive natural and discriminative instance descriptions. To address fine-grained ambiguity, we cluster seman-

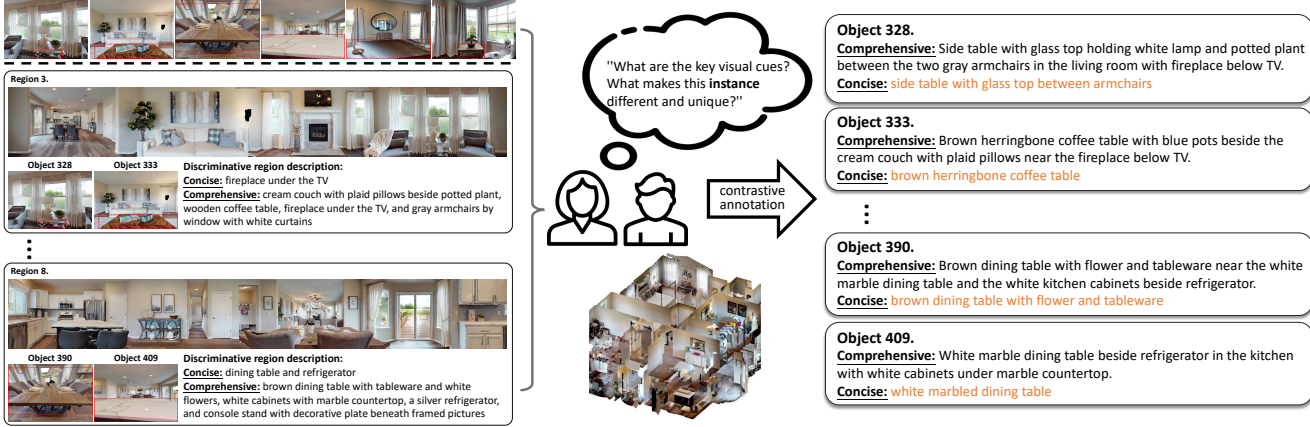


Figure 7. Contrastive instance annotation. Using object views, region panoramas, verified region descriptions, and the 3D scene, annotators write concise and detailed descriptions to distinguish each instance from others of the same category. All annotations are cross-checked.

tically similar categories using SentenceBERT [63] and refine them into a hierarchy where base categories group related fine-grained categories, *e.g.*, *yoga mat* and *gym mat* under *exercise mat*. As shown in Fig. 7, annotators select a base category and view all instances from the grouped fine-grained categories, along with object snapshots, labeled region panoramas, and verified region descriptions. They identify salient visual cues to compose one concise and one comprehensive description per instance, distinguishing it from others of the same category. The descriptions include intrinsic attributes (*e.g.*, color, material, pattern, shape, size), spatial context (*e.g.*, relative position, room or region context), and open-world semantics (*e.g.*, Eiffel Tower photo).

3.5. Navigation Task Generation

LangMap provides single- and multi-goal tasks spanning multiple semantic levels. A single-goal task consists of a scene, the agent’s start pose, and a language instruction specifying a goal at any semantic level, which may correspond to one or more target instances. A multi-goal task extends this setup with a sequence of instructions across different semantic levels, requiring the agent to reach multiple goals sequentially within a single episode.

Scene-level (category-level) instruction generation follows [1, 2], but we iterate over all object categories instead of random sampling to prevent duplication. For each category, we randomly sample a start pose subject to two constraints: (1) at least one target instance lies on the same floor to avoid stair climbing [1, 2, 7]; and (2) the geodesic distance to the nearest goal is 5–30 m (relaxed to at least 1 m if no valid pose exists). For room-level navigation, we restrict targets to instances of the specified category within the given room by intersecting region–object mappings from HM3D-Sem [10] with our human-verified region labels.

For region-level navigation, goals are further constrained by both the room type and the corresponding discriminative region description. For instance-level navigation, discriminative instance descriptions directly serve as instructions. This process yields about 15k non-redundant single-goal tasks across all four semantic levels. For multi-goal task generation, we uniformly sample five tasks across multiple semantic levels on the same floor with non-overlapping targets and concatenate them into sequential episodes, yielding 720 episodes (3.6k individual tasks).

4. Experiments

4.1. Metrics

Following prior work [1, 7, 8, 64, 65], we adopt standard evaluation protocols, reporting Success Rate (SR) and Success weighted by Path Length (SPL) as the primary metrics. SR is the fraction of tasks where the agent stops within 1m of the target within 500 steps, and SPL further accounts for path efficiency relative to the optimal trajectory:

$$SR = \frac{1}{N} \sum_{i=1}^N S_i, \quad (1)$$

$$SPL = \frac{1}{N} \sum_{i=1}^N S_i \frac{L_i^*}{\max(L_i, L_i^*)}, \quad (2)$$

where $S_i = 1$ if the i -th task succeeds and 0 otherwise, and L_i and L_i^* denote the executed and optimal path lengths.

Per-goal metrics alone struggle to capture multi-goal reliability. An agent can achieve reasonable per-goal SR yet fail to complete full episodes, since any missed sub-goal breaks the sequence, making partial success insufficient for real-world use (*e.g.*, finding a cup but failing to reach the coffee machine). We therefore additionally report Sequence Success Rate (SeqSR@ n) for multi-goal episodes, which

Table 2. Evaluation on LangMap. We report performance at each semantic level and the overall average for single-goal navigation. For region- and instance-level goals, concise descriptions are used to reflect real-world goal expressions. For multi-goal navigation, we present both sequence-level (SeqSR and SeqSR-4) and per-goal (SR and SPL) results. For 3D-Mem, results are reported using 7B and 3B open-source VLMs [49]. Uni-NaVid and MTU3D are evaluated twice, and the results are averaged.

Method	Object				Room		Region		Instance		Overall		Multi-Goal			
	SR↑	SPL↑	SR↑	SPL↑	SeqSR↑	SeqSR-4↑	SR↑	SPL↑								
PSL [8] [ECCV2024]	6.0	1.4	6.6	1.9	7.3	2.1	6.4	1.9	6.6	1.8	0.0	0.0	8.1	5.7		
SenseAct-Mono [7] [CVPR2024]	10.2	5.6	8.3	4.4	8.5	4.3	7.7	4.0	8.7	4.6	0.1	0.6	15.5	8.4		
3D-Mem-3B [64] [CVPR2025]	20.7	3.7	20.3	4.0	13.4	2.3	10.2	1.8	15.3	2.8	0.0	0.3	20.4	11.3		
3D-Mem-7B [64] [CVPR2025]	21.3	8.4	18.8	8.1	21.7	8.8	22.7	9.2	21.2	8.7	0.7	7.8	36.8	21.2		
Uni-Navid [55] [RSS2025]	33.8	16.2	33.2	16.5	30.1	15.5	26.2	13.8	30.3	15.3	0.8	6.0	34.1	12.8		
MTU3D [65] [ICCV2025]	33.1	16.7	31.4	15.9	32.7	16.5	23.8	13.3	29.7	15.4	1.5	12.4	41.4	24.5		

Table 3. Quantitative comparison of annotation discriminability via one-to-many text-to-view matching (Qwen3-VL-235B). *Exclusive Win*: instances correctly matched only by the benchmark.

Benchmark	Avg. words	Accuracy (↑)	Exclusive Win (↑)
GOAT-Bench [7]	21.1	55.9%	5.3%
LangMap (Ours)	5.2	79.7%	29.1%

measures the fraction of episodes where at least n out of K_j tasks are successfully completed in the correct order:

$$\text{SeqSR}@n = \frac{1}{M} \sum_{j=1}^M \mathbb{I} \left(\sum_{k=1}^{K_j} S_{j,k} \geq n \right), \quad (3)$$

where M is the number of multi-goal episodes, K_j is the number of tasks in episode j , and $S_{j,k}$ indicates the success of the k -th task. Each episode contains $K_j = 5$ tasks; SeqSR denotes full completion, while SeqSR-4 measures partial completion with at least four successful tasks.

4.2. Annotation Quality Analysis

To quantify discriminability, we perform one-to-many text-to-view matching on overlapping instances using Qwen3-VL-235B [66]. We restrict the comparison to instance descriptions, as region annotations are unique to LangMap. As shown in Table 3, LangMap achieves **79.7%** accuracy with *4× fewer words* (vs 55.9% for GOAT-Bench) and maintains non-inferiority in **94.7%** of cases, demonstrating the superior precision of our annotations.

4.3. Main Results

We evaluate recent advances on LangMap, including MTU3D [65], Uni-Navid [55], 3D-Mem [64], SenseAct-NN Monolithic [7], and PSL [8]. Table 2 reports their performance on single-goal navigation across semantic levels and multi-goal navigation with mixed semantic levels.

Overall Performance Analysis. MTU3D and Uni-Navid are trained on million-scale multimodal data, while 3D-Mem is training-free and relies on frozen VLMs. Among them, PSL shows the weakest results, 3D-Mem achieves moderate performance, and MTU3D and Uni-Navid lead overall. Most models perform better at coarser semantic levels (object, room, and region) than at the instance level, which involves a single target and requires stronger disambiguation. In multi-goal navigation, all methods show improved performance compared to single-goal navigation, benefiting from implicit temporal encoding or explicit memory mechanisms. Nevertheless, the low SeqSR exposes a critical reliability gap, indicating that completing all goals within a multi-goal episode remains challenging.

PSL [8] leverages CLIP [46] for vision-language alignment and trains a policy network for navigation. While it performs well on closed-set benchmarks [2, 3], it underperforms on our multi-granularity open-vocabulary benchmark. CLIP exhibits limitations in compositional reasoning [67], such as handling object relations and attribute-object bindings [68, 69], which are essential for fine-grained 3D semantic reasoning. Furthermore, training on a limited set of categories restricts PSL’s ability to generalize to open-vocabulary and compositional goals.

3D-Mem [64] is a training-free method that uses frozen VLMs for semantic reasoning and maintains explicit memory of the explored environment. For fair evaluation, we use the open-source Qwen2.5-VL-7B and -3B [49], as closed-source models like GPT-4o are orders of magnitude larger and prohibitively expensive for deployment. As shown in Table 2, 3D-Mem-3B performs comparably to 3D-Mem-7B on object- and room-level navigation, which mainly rely on perception and detection, but underperforms on region- and instance-level navigation, where success depends on fine-grained semantic and relational reasoning. While 3D-Mem outperforms PSL, it incurs high latency (about 2.5 min per task) and trails models trained on large-scale multimodal navigation data. However, with explicit memory of detected

Table 4. Ablation of description styles. Concise descriptions are used by default. ‘-D’ denotes using detailed descriptions.

Method	Region		Region-D		Instance		Instance-D	
	SR↑	SPL↑	SR↑	SPL↑	SR↑	SPL↑	SR↑	SPL↑
PSL	7.3	2.1	9.0	2.6	6.4	1.9	8.5	2.4
3D-Mem	21.7	8.8	25.4	8.5	22.7	9.2	25.7	9.6
Uni-NaVid	30.1	15.5	31.7	17.4	26.2	13.8	28.8	15.9
MTU3D	32.7	16.5	33.7	16.2	23.8	13.3	28.7	15.2

Table 5. Ablation of head (top 20%) and long-tail object categories.

Method	Head		Long-tail	
	SR↑	SPL↑	SR↑	SPL↑
PSL	7.3	2.0	4.4	1.1
3D-Mem	21.5	9.1	20.2	7.3
Uni-NaVid	31.3	15.9	26.1	13.2
MTU3D	31.5	16.3	23.0	12.2

Table 6. Ablation of object visibility. Small (<3.3% mean IoU).

Method	Non-small		Small	
	SR↑	SPL↑	SR↑	SPL↑
PSL	7.2	2.0	4.6	1.3
3D-Mem	22.1	9.2	17.0	6.6
Uni-NaVid	32.6	16.5	23.0	10.9
MTU3D	32.7	16.8	20.0	10.1

Table 7. Ablation of optimal path lengths. Short ($\leq 25\%$), medium (25–75%), and long ($> 75\%$).

Method	Short		Medium		Long		Overall	
	SR↑	SPL↑	SR↑	SPL↑	SR↑	SPL↑	SR↑	SPL↑
PSL	13.4	3.2	5.4	1.6	2.3	0.8	6.6	1.8
3D-Mem	36.7	17.1	19.8	7.3	8.8	3.2	21.2	8.7
Uni-NaVid	42.2	21.5	29.7	14.7	19.4	10.3	30.3	15.3
MTU3D	47.2	22.2	27.9	15.2	15.9	9.1	29.7	15.4

objects and accumulated spatial context, it achieves competitive performance in multi-goal navigation.

Uni-NaVid [55] is a VLM-based model trained on 3.6 million navigation samples across multiple tasks. It predicts low-level actions directly from language and egocentric RGB streams without using depth information, enabling lightweight and practical deployment. **MTU3D** [65] performs end-to-end trajectory learning that combines vision-language-exploration pre-training over 1 million RGB-D trajectories. Both methods achieve top-tier performance on LangMap, benefiting from large-scale multimodal training that enhances temporal and spatial–semantic reasoning. Uni-NaVid shows a marginally higher SR (+0.6%) in single-goal navigation. However, MTU3D performs notably better on multi-goal sequence tasks due to its explicit memory of explored objects for decision making.

4.4. Ablation Study

Description Style. In Table 4, we evaluate the impact of description style on navigation performance. Unless otherwise specified, 3D-Mem refers to 3D-Mem-7B. For both region- and instance-level goals, detailed descriptions improve success rate by providing richer contextual cues that help disambiguate semantically similar targets and strengthen visual–language grounding. In contrast, concise descriptions, while containing distinctive cues, are often harder to ground reliably in visual observations.

Head vs. Long-Tail Object Categories. We partition object categories into head and long-tail groups based on their frequency in the dataset, following the Pareto principle [70]. The head group (top 20%) covers about 77% of all

tasks, while the long-tail group (remaining 80%) accounts for 23%. As shown in Table 5, all methods exhibit substantial performance drops on long-tail categories compared to head categories. Notably, 3D-Mem shows the smallest gap, benefiting from its frozen VLM that preserves broad open-world knowledge.

Object Size and Visibility. Table 6 analyzes the impact of object visibility on navigation performance. All models exhibit clear performance degradation when targets are small (mean IoU $< 3.3\%$), highlighting the difficulty of detecting and localizing small or low-visibility objects.

Path Length. We group tasks by optimal path length using the geodesic distance distribution in Fig. 6(b), with the 25th and 75th percentiles defining short ($\leq 25\%$), medium (25–75%), and long ($> 75\%$) ranges. As shown in Table 7, performance decreases as target distance increases, reflecting the challenge of long-horizon exploration. Uni-NaVid and MTU3D show the most stable performance, benefiting from large-scale trajectory learning that enhances long-horizon decision-making.

5. Conclusion

We introduced HieraNavi, a multi-granularity open-vocabulary navigation task that unifies goals across four semantic levels, capturing the hierarchical and fine-grained distinctions essential for real-world scenarios. We presented LangMap, a large-scale benchmark built on real-world 3D scans with comprehensive human-verified annotations and navigation tasks across these levels. Compared with GOAT-Bench, LangMap achieves 23.8% higher discriminative accuracy using 4 \times fewer words, setting a new standard for high-quality and natural semantic annotations. Extensive evaluations show that although memory and large-scale multimodal training improve grounding and planning, robust reasoning over long-tailed, small, context-dependent, and distant goals, as well as multi-goal completion, remain challenging. Together, HieraNavi and LangMap establish a rigorous and standardized testbed for future research on language-conditioned goal navigation in complex real-world environments.

References

[1] N. Yokoyama, R. Ramrakhy, A. Das, D. Batra, and S. Ha, “Hm3d-ovon: A dataset and benchmark for open-vocabulary object goal navigation,” in *2024 IEEE/RSJ International Conference on Intelligent Robots and Systems (IROS)*, pp. 5543–5550, IEEE, 2024. [1](#), [2](#), [3](#), [4](#), [5](#)

[2] K. Yadav, J. Krantz, R. Ramrakhy, S. K. Ramakrishnan, J. Yang, *et al.*, “Habitat challenge 2023.” <https://aihabitat.org/challenge/2023/>, 2023. [1](#), [2](#), [3](#), [4](#), [6](#), [7](#)

[3] J. Krantz, S. Lee, J. Malik, D. Batra, and D. S. Chaplot, “Instance-specific image goal navigation: Training embodied agents to find object instances,” *arXiv preprint arXiv:2211.15876*, 2022. [1](#), [2](#), [7](#)

[4] J. Krantz, T. Gervet, K. Yadav, A. Wang, C. Paxton, R. Mottaghi, D. Batra, J. Malik, S. Lee, and D. S. Chaplot, “Navigating to objects specified by images,” in *Proceedings of the IEEE/CVF International Conference on Computer Vision*, pp. 10916–10925, 2023. [1](#), [2](#)

[5] A. Chang, A. Dai, T. Funkhouser, M. Halber, M. Niessner, M. Savva, S. Song, A. Zeng, and Y. Zhang, “Matterport3d: Learning from rgb-d data in indoor environments,” *arXiv preprint arXiv:1709.06158*, 2017. [1](#), [2](#), [3](#), [4](#)

[6] X. Song, W. Chen, Y. Liu, W. Chen, G. Li, and L. Lin, “Towards long-horizon vision-language navigation: Platform, benchmark and method,” in *Proceedings of the Computer Vision and Pattern Recognition Conference*, pp. 12078–12088, 2025. [1](#), [3](#), [4](#)

[7] M. Khanna, R. Ramrakhy, G. Chhablani, S. Yenamandra, T. Gervet, M. Chang, Z. Kira, D. S. Chaplot, D. Batra, and R. Mottaghi, “Goat-bench: A benchmark for multimodal lifelong navigation,” in *Proceedings of the IEEE/CVF Conference on Computer Vision and Pattern Recognition*, pp. 16373–16383, 2024. [1](#), [2](#), [3](#), [4](#), [5](#), [6](#), [7](#)

[8] X. Sun, L. Liu, H. Zhi, R. Qiu, and J. Liang, “Prioritized semantic learning for zero-shot instance navigation,” in *European Conference on Computer Vision*, pp. 161–178, Springer, 2024. [1](#), [2](#), [3](#), [4](#), [6](#), [7](#)

[9] S. K. Ramakrishnan, A. Gokaslan, E. Wijmans, O. Maksymets, A. Clegg, J. M. Turner, E. Undersander, W. Galuba, A. Westbury, A. X. Chang, M. Savva, Y. Zhao, and D. Batra, “Habitat-matterport 3d dataset (HM3d): 1000 large-scale 3d environments for embodied AI,” in *Thirty-fifth Conference on Neural Information Processing Systems Datasets and Benchmarks Track*, 2021. [1](#), [2](#), [3](#), [4](#)

[10] K. Yadav, R. Ramrakhy, S. K. Ramakrishnan, T. Gervet, J. Turner, A. Gokaslan, N. Maestre, A. X. Chang, D. Batra, M. Savva, *et al.*, “Habitat-matterport 3d semantics dataset,” in *Proceedings of the IEEE/CVF Conference on Computer Vision and Pattern Recognition*, pp. 4927–4936, 2023. [1](#), [2](#), [3](#), [4](#), [5](#), [6](#)

[11] Y. Li, Y. Du, K. Zhou, J. Wang, W. X. Zhao, and J.-R. Wen, “Evaluating object hallucination in large vision-language models,” *arXiv preprint arXiv:2305.10355*, 2023. [1](#), [3](#)

[12] W. Cai, I. Ponomarenko, J. Yuan, X. Li, W. Yang, H. Dong, and B. Zhao, “Spatialbot: Precise spatial understanding with vision language models,” in *2025 IEEE International Conference on Robotics and Automation (ICRA)*, pp. 9490–9498, IEEE, 2025. [1](#), [3](#)

[13] B. Chen, Z. Xu, S. Kirmani, B. Ichter, D. Sadigh, L. Guibas, and F. Xia, “Spatialvlm: Endowing vision-language models with spatial reasoning capabilities,” in *Proceedings of the IEEE/CVF Conference on Computer Vision and Pattern Recognition*, pp. 14455–14465, 2024.

[14] Q. Guo, S. De Mello, H. Yin, W. Byeon, K. C. Cheung, Y. Yu, P. Luo, and S. Liu, “Regionopt: Towards region understanding vision language model,” in *Proceedings of the IEEE/CVF Conference on Computer Vision and Pattern Recognition*, pp. 13796–13806, 2024. [3](#)

[15] B. Miao, M. Feng, Z. Wu, M. Bennamoun, Y. Gao, and A. Mian, “Referring human pose and mask estimation in the wild,” *Advances in Neural Information Processing Systems*, vol. 37, pp. 44791–44813, 2024. [1](#)

[16] P. Anderson, Q. Wu, D. Teney, J. Bruce, M. Johnson, N. Sünderhauf, I. Reid, S. Gould, and A. Van Den Hengel, “Vision-and-language navigation: Interpreting visually-grounded navigation instructions in real environments,” in *Proceedings of the IEEE conference on computer vision and pattern recognition*, pp. 3674–3683, 2018. [2](#)

[17] J. Krantz, E. Wijmans, A. Majumdar, D. Batra, and S. Lee, “Beyond the nav-graph: Vision-and-language navigation in continuous environments,” in *European Conference on Computer Vision*, pp. 104–120, Springer, 2020.

[18] A. Ku, P. Anderson, R. Patel, E. Ie, and J. Baldridge, “Room-across-room: Multilingual vision-and-language navigation with dense spatiotemporal grounding,” *arXiv preprint arXiv:2010.07954*, 2020. [2](#)

[19] P. Anderson, A. Chang, D. S. Chaplot, A. Dosovitskiy, S. Gupta, V. Koltun, J. Kosecka, J. Malik, R. Mottaghi, M. Savva, *et al.*, “On evaluation of embodied navigation agents,” *arXiv preprint arXiv:1807.06757*, 2018. [2](#)

[20] D. S. Chaplot, D. Gandhi, S. Gupta, A. Gupta, and R. Salakhutdinov, “Learning to explore using active neural slam,” *ICLR*, 2020. [2](#)

[21] X. Zhao, H. Agrawal, D. Batra, and A. G. Schwing, “The surprising effectiveness of visual odometry techniques for embodied pointgoal navigation,” in *Proceedings of the IEEE/CVF International Conference on Computer Vision*, pp. 16127–16136, 2021.

[22] R. Partsey, E. Wijmans, N. Yokoyama, O. Dobosevych, D. Batra, and O. Maksymets, “Is mapping necessary for realistic pointgoal navigation?,” in *Proceedings of the IEEE/CVF Conference on Computer Vision and Pattern Recognition*, pp. 17232–17241, 2022. [2](#)

[23] D. S. Chaplot, D. P. Gandhi, A. Gupta, and R. R. Salakhutdinov, “Object goal navigation using goal-oriented semantic exploration,” *Advances in Neural Information Processing Systems*, vol. 33, pp. 4247–4258, 2020. [2](#)

[24] D. Batra, A. Gokaslan, A. Kembhavi, O. Maksymets, R. Mottaghi, M. Savva, A. Toshev, and E. Wijmans, “Object-nav revisited: On evaluation of embodied agents navigating to objects,” *arXiv preprint arXiv:2006.13171*, 2020.

[25] J. Zhang, L. Dai, F. Meng, Q. Fan, X. Chen, K. Xu, and H. Wang, “3d-aware object goal navigation via simultaneous exploration and identification,” in *Proceedings of the IEEE/CVF Conference on Computer Vision and Pattern Recognition*, pp. 6672–6682, 2023.

[26] S. Y. Gadre, M. Wortsman, G. Ilharco, L. Schmidt, and S. Song, “Cows on pasture: Baselines and benchmarks for language-driven zero-shot object navigation,” in *Proceedings of the IEEE/CVF Conference on Computer Vision and Pattern Recognition*, pp. 23171–23181, 2023. 3

[27] J. Chen, G. Li, S. Kumar, B. Ghanem, and F. Yu, “How to not train your dragon: Training-free embodied object goal navigation with semantic frontiers,” in *Proceedings of Robotics: Science and Systems (RSS)*, 2023.

[28] S. Wani, S. Patel, U. Jain, A. X. Chang, and M. Savva, “Multion: Benchmarking semantic map memory using multi-object navigation,” in *Advances in Neural Information Processing Systems (NeurIPS)*, 2020. 2

[29] Y. Zhu, R. Mottaghi, E. Kolve, J. J. Lim, A. Gupta, L. Fei-Fei, and A. Farhadi, “Target-driven visual navigation in indoor scenes using deep reinforcement learning,” in *2017 IEEE international conference on robotics and automation (ICRA)*, pp. 3357–3364, IEEE, 2017. 2

[30] N. Kim, O. Kwon, H. Yoo, Y. Choi, J. Park, and S. Oh, “Topological semantic graph memory for image-goal navigation,” in *Conference on Robot Learning*, pp. 393–402, PMLR, 2023.

[31] X. Sun, P. Chen, J. Fan, J. Chen, T. Li, and M. Tan, “Fg-prompt: fine-grained goal prompting for image-goal navigation,” *Advances in Neural Information Processing Systems*, vol. 36, pp. 12054–12073, 2023. 2

[32] E. Wijmans, A. Kadian, A. Morcos, S. Lee, I. Essa, D. Parikh, M. Savva, and D. Batra, “Dd-ppo: Learning near-perfect pointgoal navigators from 2.5 billion frames,” in *International Conference on Learning Representations (ICLR)*, 2020. 2

[33] A. Mousavian, A. Toshev, M. Fišer, J. Košecká, A. Wahid, and J. Davidson, “Visual representations for semantic target driven navigation,” in *International Conference on Robotics and Automation (ICRA)*, pp. 8846–8852, 2019.

[34] J. Ye, D. Batra, A. Das, and E. Wijmans, “Auxiliary tasks and exploration enable objectgoal navigation,” in *Proceedings of the IEEE/CVF International Conference on Computer Vision (ICCV)*, pp. 16117–16126, IEEE, 2021.

[35] Y. Hong, Q. Wu, Y. Qi, C. Rodriguez-Opazo, and S. Gould, “Vln-bert: A recurrent vision-and-language bert for navigation,” in *Proceedings of the IEEE/CVF Conference on Computer Vision and Pattern Recognition (CVPR)*, pp. 1643–1653, 2021.

[36] R. Ramrakhy, D. Batra, E. Wijmans, and A. Das, “Pirlnav: Pretraining with imitation and rl finetuning for objectnav,” in *Proceedings of the IEEE/CVF Conference on Computer Vision and Pattern Recognition (CVPR)*, pp. 17896–17906, 2023.

[37] E. Wijmans, I. Essa, and D. Batra, “Ver: Scaling on-policy rl leads to the emergence of navigation in embodied rearrangement,” in *Advances in Neural Information Processing Systems (NeurIPS)*, vol. 35, pp. 7727–7740, 2022.

[38] K.-H. Zeng, Z. Zhang, K. Ehsani, R. Hendrix, J. Salvador, A. Herrasti, R. B. Girshick, A. Kembhavi, and L. Weihs, “Poliformer: Scaling on-policy rl with transformers results in masterful navigators,” *arXiv preprint arXiv:2406.20083*, June 2024. 2

[39] B. Yu, H. Kasaei, and M. Cao, “Frontier semantic exploration for visual target navigation,” in *IEEE International Conference on Robotics and Automation (ICRA)*, pp. 4099–4105, 2023. 2

[40] N. Yokoyama, S. Ha, D. Batra, J. Wang, and B. Bucher, “Vlfm: Vision-language frontier maps for zero-shot semantic navigation,” in *Proceedings of the IEEE/RSJ International Conference on Robotics and Automation (ICRA)*, 2024.

[41] F. Xie, S. Schwertfeger, and H. Blum, “osmag-llm: Zero-shot open-vocabulary object navigation via semantic maps and large language models reasoning,” *IEEE Robotics and Automation Letters*, vol. 11, no. 3, pp. 2426–2433, 2026.

[42] B. Sun, H. Chen, S. Leutenegger, C. Cadena, M. Pollefeys, and H. Blum, “Frontiernet: Learning visual cues to explore,” *IEEE Robotics and Automation Letters*, 2025. 2

[43] A. Pal, Y. Qiu, and H. I. Christensen, “Learning hierarchical relationships for object-goal navigation,” in *Proceedings of the Conference on Robot Learning (CoRL)*, vol. 164, pp. 517–528, PMLR, 2021. 3

[44] S. K. Ramakrishnan, D. S. Chaplot, Z. Al-Halah, J. Malik, and K. Grauman, “Poni: Potential functions for objectgoal navigation with interaction-free learning,” in *Proceedings of the IEEE/CVF Conference on Computer Vision and Pattern Recognition (CVPR)*, pp. 18890–18900, 2022. 3

[45] G. Georgakis, B. Bucher, K. Schmeckpeper, S. Singh, and K. Daniilidis, “Learning to map for active semantic goal navigation,” in *International Conference on Learning Representations (ICLR)*, 2022. 3

[46] A. Radford, J. W. Kim, C. Hallacy, A. Ramesh, G. Goh, S. Agarwal, G. Sastry, A. Askell, P. Mishkin, J. Clark, G. Krueger, and I. Sutskever, “Learning transferable visual models from natural language supervision,” in *Proceedings of the International Conference on Machine Learning (ICML)*, vol. 139, pp. 8748–8763, 2021. 3, 7

[47] OpenAI, “Gpt-4o system card,” *arXiv preprint arXiv:2410.21276*, 2024.

[48] H. Liu, C. Li, Q. Wu, and Y. J. Lee, “Visual instruction tuning: Large language and vision assistant,” in *Advances in Neural Information Processing Systems (NeurIPS)*, 2023.

[49] S. Bai, K. Chen, X. Liu, J. Wang, W. Ge, S. Song, K. Dang, P. Wang, S. Wang, J. Tang, and et al., “Qwen2.5-vl technical report,” *arXiv preprint arXiv:2502.13923*, 2025. 7

[50] W.-L. Chiang, Z. Li, Z. Lin, Y. Sheng, Z. Wu, H. Zhang, L. Zheng, S. Zhuang, Y. Zhuang, J. E. Gonzalez, et al., “Vicuna: An open-source chatbot impressing gpt-4 with 90%* chatgpt quality,” See <https://vicuna.lmsys.org> (accessed 14 April 2023), vol. 2, no. 3, p. 6, 2023. 3

[51] A. Majumdar, G. Aggarwal, B. Devnani, J. Hoffman, and D. Batra, “Zson: Zero-shot object-goal navigation using multimodal goal embeddings,” in *Advances in Neural Information Processing Systems (NeurIPS)*, vol. 35, 2022. 3

[52] B. Chen, F. Xia, B. Ichter, K. Rao, K. Gopalakrishnan, M. S. Ryoo, A. Stone, and D. Kappler, “Open-vocabulary queryable scene representations for real world planning,” *arXiv preprint arXiv:2209.09874*, September 2022.

[53] K. Zhou, K. Zheng, C. Pryor, Y. Shen, H. Jin, L. Getoor, and X. E. Wang, “Esc: Exploration with soft commonsense constraints for zero-shot object navigation,” in *Proceedings of the International Conference on Machine Learning (ICML)*, vol. 202 of *Proceedings of Machine Learning Research*, pp. 42829–42842, 2023.

[54] Y. Long, W. Cai, H. Wang, G. Zhan, and H. Dong, “Instructnav: Zero-shot system for generic instruction navigation in unexplored environments,” in *Proceedings of the Conference on Robot Learning (CoRL)*, vol. 270, pp. 2049–2060, 2025.

[55] J. Zhang, K. Wang, S. Wang, M. Li, H. Liu, S. Wei, Z. Wang, Z. Zhang, and H. Wang, “Uni-navid: A video-based vision-language-action model for unifying embodied navigation tasks,” *Robotics: Science and Systems*, 2025. 7, 8

[56] H. Yin, X. Xu, L. Zhao, Z. Wang, J. Zhou, and J. Lu, “Unigoal: Towards universal zero-shot goal-oriented navigation,” in *Proceedings of the Computer Vision and Pattern Recognition Conference*, pp. 19057–19066, 2025. 3

[57] M. Deitke, W. Han, A. Herrasti, A. Kembhavi, E. Kolve, R. Mottaghi, J. Salvador, D. Schwenk, E. VanderBilt, M. Wallingford, *et al.*, “Robothor: An open simulation-to-real embodied ai platform,” in *Proceedings of the IEEE/CVF conference on computer vision and pattern recognition*, pp. 3164–3174, 2020. 4

[58] M. Deitke, E. VanderBilt, A. Herrasti, L. Weihs, K. Ehsani, J. Salvador, W. Han, E. Kolve, A. Kembhavi, and R. Mottaghi, “Proctor: Large-scale embodied ai using procedural generation,” *Advances in Neural Information Processing Systems*, vol. 35, pp. 5982–5994, 2022. 3

[59] S. Yenamandra, A. Ramachandran, K. Yadav, A. Wang, M. Khanna, T. Gervet, T.-Y. Yang, V. Jain, A. W. Clegg, J. Turner, *et al.*, “Homerobot: Open-vocabulary mobile manipulation,” *arXiv preprint arXiv:2306.11565*, 2023. 3

[60] M. Khanna, Y. Mao, H. Jiang, S. Hares, B. Shacklett, D. Batra, A. Clegg, E. Undersander, A. X. Chang, and M. Savva, “Habitat synthetic scenes dataset (hssd-200): An analysis of 3d scene scale and realism tradeoffs for objectgoal navigation,” in *Proceedings of the IEEE/CVF Conference on Computer Vision and Pattern Recognition (CVPR)*, pp. 16384–16393, June 2024. 3

[61] C. C. Kemp, A. Edsinger, H. M. Clever, and B. Matulevich, “The design of stretch: A compact, lightweight mobile manipulator for indoor human environments,” in *2022 International Conference on Robotics and Automation (ICRA)*, pp. 3150–3157, IEEE, 2022. 4

[62] J. Achiam, S. Adler, S. Agarwal, L. Ahmad, I. Akkaya, F. L. Aleman, D. Almeida, J. Altenschmidt, S. Altman, S. Anadkat, and et al., “Gpt-4 technical report,” *arXiv preprint arXiv:2303.08774*, 2023. 5

[63] N. Reimers and I. Gurevych, “Sentence-bert: Sentence embeddings using siamese bert-networks,” *arXiv preprint arXiv:1908.10084*, 2019. 6

[64] Y. Yang, H. Yang, J. Zhou, P. Chen, H. Zhang, Y. Du, and C. Gan, “3d-mem: 3d scene memory for embodied exploration and reasoning,” in *Proceedings of the Computer Vision and Pattern Recognition Conference*, pp. 17294–17303, 2025. 6, 7

[65] Z. Zhu, X. Wang, Y. Li, Z. Zhang, X. Ma, Y. Chen, B. Jia, W. Liang, Q. Yu, Z. Deng, *et al.*, “Move to understand a 3d scene: Bridging visual grounding and exploration for efficient and versatile embodied navigation,” in *Proceedings of the IEEE/CVF International Conference on Computer Vision*, pp. 8120–8132, 2025. 6, 7, 8

[66] S. Bai, Y. Cai, R. Chen, K. Chen, X. Chen, Z. Cheng, L. Deng, W. Ding, C. Gao, C. Ge, W. Ge, Z. Guo, Q. Huang, J. Huang, F. Huang, B. Hui, S. Jiang, Z. Li, M. Li, M. Li, K. Li, Z. Lin, J. Lin, X. Liu, J. Liu, C. Liu, Y. Liu, D. Liu, S. Liu, D. Lu, R. Luo, C. Lv, R. Men, L. Meng, X. Ren, X. Ren, S. Song, Y. Sun, J. Tang, J. Tu, J. Wan, P. Wang, P. Wang, Q. Wang, Y. Wang, T. Xie, Y. Xu, H. Xu, J. Xu, Z. Yang, M. Yang, J. Yang, A. Yang, B. Yu, F. Zhang, H. Zhang, X. Zhang, B. Zheng, H. Zhong, J. Zhou, F. Zhou, J. Zhou, Y. Zhu, and K. Zhu, “Qwen3-vl technical report,” *arXiv preprint arXiv:2511.21631*, 2025. 7

[67] T. Thrush, R. Jiang, M. Bartolo, A. Singh, A. Williams, D. Kiela, and C. Ross, “Winoground: Probing vision and language models for visio-linguistic compositionality,” in *Proceedings of the IEEE/CVF Conference on Computer Vision and Pattern Recognition*, pp. 5238–5248, 2022. 7

[68] A. Kamath, J. Hessel, and K.-W. Chang, “Text encoders bottleneck compositionality in contrastive vision-language models,” in *Proceedings of the 2023 Conference on Empirical Methods in Natural Language Processing*, pp. 4933–4944, 2023. 7

[69] M. Yuksekgonul, F. Bianchi, P. Kalluri, D. Jurafsky, and J. Zou, “When and why vision-language models behave like bags-of-words, and what to do about it?,” *arXiv preprint arXiv:2210.01936*, 2022. 7

[70] V. Pareto, *Cours d'économie politique*, vol. 1. Librairie Droz, 1964. 8